Effect and applications of patterned laser illumination on superconducting films

C. C. Chi, M. M. T. Loy, and D. C. Cronemeyer
IBM Thomas J. Watson Research Center, Yorktown Heights, New York 10598
(Received 7 November 1983)

Patterned laser illumination incident upon superconducting films is shown to be capable of creating dynamic superconducting-normal (S-N) interfaces with almost any desired pattern. The width of such a dynamic interface for a sharp illumination edge is shown to be the effective quasiparticle diffusion length. In the limit of strong phonon trapping in the film, the effective quasiparticle diffusion length approaches the thermal healing length obtained from the heat diffusion model. However, this is not the appropriate limit in general for thin films immersed in liquid helium. The ability to create dynamic S-N patterns can be used in probing spatial inhomogeneity of superconducting films and tunnel junctions. An Al-Al_2O_3-Pb junction was used to demonstrate the technique. For the first time, the spatial distribution of tunneling probability was obtained through the measurements of local Josephson current. It is shown that this is a much more reliable technique than attempting to infer the tunneling probability from the excess quasiparticle tunneling current due to a local laser or electron beam excitation.

I. INTRODUCTION

In the past decade laser light has frequently been used to perturb superconductors out of thermal equilibrium in order to study various relaxation times and nonequilibrium phenomena.[1] Recently, there has been a surge of interest in using either laser light[2,3] or electron-beam[4–7] excitation to probe the spatial inhomogeneity of the superconducting properties of thin films and tunnel junctions. The most important virtue of using either laser light or electron-beam excitation is that of being able to perturb the superconducting film locally. However, the ultimate spatial resolution of these probing techniques depends on how far the localized perturbation actually spreads out into the unperturbed region.

To use the electron-beam scanning technique, the superconducting sample must be mounted on a cold finger in vacuum. Owing to the bottleneck of removing phonons from the superconducting film, the effect of an electron beam was considered to be simple heating, and the spatial resolution was considered to be the thermal healing length obtained from the classical heat-diffusion equation.[7,8] The situation for laser light probing, on the other hand, may be quite different. The sample can be immersed in superfluid He to improve the phonon-removal rate from the film. For thin superconducting films, it is not clear that the thermal healing length is the proper length scale. In Sec. II A of this paper, this question is explored with the use of Rothwarf-Taylor phenomenological equations. The effective quasiparticle diffusion length is shown to be the proper length scale, which approaches the classical thermal healing length in the limit of a severe phonon bottleneck condition. Different functional forms of quasiparticle diffusion from the perturbed region into the unperturbed region were obtained for weak and strong perturbations. In Sec. II B, a superconducting tunnel junction of Al-Al_2O_3-Pb was used to measure the spatial resolution of a particular optical projection system, the overall resolution in this case is shown to be about 5 μm, which is limited by the optical resolution rather than by the effective quasiparticle diffusion.

The optical projection system used in this experiment is capable of two different kinds of probing. The first one is to probe wherever the sample is perturbed, and the second one is complementary to the first, i.e., to probe wherever the sample is not perturbed.[3] For the first method, the perturbed region is confined to a small spot. Some electrical signals can be obtained as a function of the position of the perturbed spot. Since the signals were due to a perturbed region, the result is subject to the nonequilibrium relaxation processes. The second method measures the superconducting properties of the dark region by using laser projection to drive the unprobed surrounding region normal. Since the signal comes from the unperturbed region, the result is not subject to the relaxation processes. In Sec. III we demonstrate the use of the optical projection system for both methods with Al-Al_2O_3-Pb tunnel junctions. Various distributions of superconducting parameters, such as T_c and I_c, were obtained for Al. For the first time, a distribution of tunneling probability was obtained. We have also shown that the excess quasiparticle current of the tunnel junction due to a small spot perturbation of light (or electrons) cannot be used to infer the tunneling probability without extreme caution. Finally, the main results of this work are summarized in Sec. IV, with a brief discussion of extendability and limitations of these probing techniques.

II. DYNAMIC INTERFACES

A. Theory

Let us consider a simple situation where half of a thin superconducting film is illuminated uniformly and the other half is dark. Let us further assume the illumination edge is absolutely sharp. It is obvious that well within the

dark region the film is in thermal equilibrium at the ambient temperature T, while well within the illuminated region the densities of quasiparticles and phonons reach certain steady state values which are higher than those for thermal equilibrium. To find out rigorously how wide the transition region is, one needs to solve the Boltzmann equations for the quasiparticles and the phonons. It has been shown that the phenomenological Rothwarf-Taylor (RT) equations[9] are a good approximation for the Boltzmann equation as long as one is not interested in the detailed energy distributions of quasiparticles and phonons.[10] Since it is easier to obtain a useful physical picture of the dynamic interface problem with the RT equations, we take this approach rather than using the more elaborate Boltzmann-equation approach. The RT equations with quasiparticle- and phonon-diffusion terms can be written as

$$\dot{n}_q = -Rn_q^2 + 2n_{\rm ph}\tau_B^{-1} + D_q\nabla^2 n_q + I_q \ , \tag{1}$$

$$\dot{n}_{\rm ph} = (Rn_q^2/2) - n_{\rm ph}\tau_B^{-1} + D_p\nabla^2 n_{\rm ph} - (n_{\rm ph} - n_{{\rm ph}\,T})\tau_\gamma^{-1} + I_{\rm ph} \ , \tag{2}$$

where n_q and $n_{\rm ph}$ are the quasiparticle and phonon densities, D_q and $D_{\rm ph}$ are the quasiparticle and phonon diffusivities, respectively. I_q and $I_{\rm ph}$ are the quasiparticle and phonon generation rates due to optical illumination, R is the quasiparticle recombination constant, τ_B^{-1} is the phonon pair-breaking rate, and τ_γ^{-1} is the phonon thermalization rate with the thermal bath (substrate and helium bath). The approximations involved in obtaining the RT equations from the general Boltzman equation are as follows: (a) the low-energy phonons with energy insufficient to break a Cooper pair are ignored, (b) the various rate constants, i.e., $R, \tau_B^{-1}, \tau_\gamma^{-1}$, are assumed to be independent of the detailed energy distribution of quasiparticles and phonons, and (c) the cascading processes of the photon-excited high-energy quasiparticles are replaced by the effective quasiparticles and phonon source terms I_q and $I_{\rm ph}$, which can be chosen to approximate the end result of the fast cascading processes.[11]

As is usually the case for metals, the quasiparticle diffusion constant D_q is much larger than the phonon diffusion constant $D_{\rm ph}$ so that the latter can be omitted in Eq. (2). Then with some manipulation, the steady-state solution of Eqs. (1) and (2) can be written as

$$-R^{\rm eff}(n_q^2 - n_{q\,T}^2) + D\nabla^2 n_q + I_q^{\rm eff} = 0 \ , \tag{3}$$

$$-(n_{\rm ph} - n_{{\rm ph}\,T})\tau_\gamma^{-1} + D\nabla^2 n_q/2 + I_{\rm ph}^{\rm eff} = 0 \ , \tag{4}$$

where

$$D \equiv D_q, \ R^{\rm eff} \equiv R/(1+\tau_\gamma/\tau_B) \ ,$$

$$I_q^{\rm eff} \equiv I_q + 2I_p/(1+\tau_B/\tau_\gamma) \ ,$$

and $I_{\rm ph}^{\rm eff} = I_{\rm ph} + I_q/2$. The thermal equilibrium values of n_{qT} and $n_{{\rm ph}\,T}$ obey the following relationship:

$$Rn_{q\,T}^2 = 2n_{{\rm ph}\,T}\tau_B^{-1} \ . \tag{5}$$

Equations (3) and (4) can be readily used to obtain the steady-state values of quasiparticles and phonons far away from the transition region, which is defined as the vicinity near $x=0$:

$$\begin{aligned} n_{q-} &\equiv n_q(-\infty) = n_{q\,T} \ , \\ n_{{\rm ph}-} &\equiv n_{\rm ph}(-\infty) = n_{{\rm ph}\,T} \ , \\ n_{q+} &\equiv n_q(+\infty) = (n_{q\,T}^2 + I_q^{\rm eff}/R^{\rm eff})^{1/2} \ , \\ n_{{\rm ph}+} &\equiv n_{\rm ph}(+\infty) = n_{{\rm ph}\,T} + I_{\rm ph}^{\rm eff}\tau_\gamma \ . \end{aligned} \tag{6}$$

Then Eqs. (3) and (4) can be reduced to

$$-R^{\rm eff}(n_q^2 - n_{q\pm}^2) + D\,d^2 n_q/dx^2 = 0 \ , \tag{7}$$

$$-(n_{\rm ph} - n_{{\rm ph}\pm})\tau_\gamma^{-1} + (D/2)\,d^2 n_q/dx^2 = 0 \ , \tag{8}$$

where the subscripts $+$ and $-$ indicate the region of $x>0$ and $x<0$, respectively. Equation (7) can be linearized to the standard one-dimensional diffusion equation if the light intensity is weak, i.e., $(n_q - n_{q\pm}) \ll n_{q\,T}$. Then the solution of n_q can be given as

$$n_q(x) = n_{q\pm} \mp \tfrac{1}{2}(n_{q+} - n_{q-})e^{-|x|/\Lambda} \ , \tag{9}$$

$$\Lambda \equiv (D/2n_{qT}R^{\rm eff})^{1/2} \ . \tag{10}$$

When the light intensity is strong or the bath temperature is low, i.e., $n_{q+} \gg n_{q\,T}$, then the solution of Eq. (8) in the dark region near the illumination interface can be given as

$$n_q(x) - n_{qT} = \frac{6D/R^{\rm eff}n_{q\,T}}{(x+x_0)^2} \quad \text{for } x<0 \ . \tag{11}$$

The constant x_0 can be determined by matching this dark-region solution to that on the illuminated side, i.e., $x>0$. The interesting point is that the quasiparticle density decreases from the interface as a power law instead of an exponential until $n_q(x)$ becomes comparable to n_{qT}. The length scale in this case is $(6D/R^{\rm eff}n_{qT})^{1/2}$, which is of the same order of magnitude as the exponential decay length given by Eq. (10). Therefore, except for the detailed functional form, we expect that the length scale of the transition region is always 2Λ, regardless of the light intensity.

It is appropriate at this point to note that this treatment of diffusion at the boundary between dark and light regions is more general than the treatment using the classical heat-diffusion equation, in which a local thermal equilibrium among quasiparticles and phonons is assumed. As a matter of fact, in the limit of $\tau_\gamma \gg \tau_B$, the quasiparticle diffusion length given by Eq. (10) approaches the thermal healing length l_T obtained from the heat-diffusion equation, where l_T is given by:[8]

$$l_T \equiv (Kd/\alpha)^{1/2} \tag{12}$$

and K is the thermal conductance of the film, d is the film thickness, and α is the Kapitza conductance of the film-He and/or film-substrate interfaces. The equality between Λ and l_T can be established by noting that $K \sim n_{q\,T}Dk_B$, $\alpha \sim \eta n_{{\rm ph}\,T}V_s k_B$, and $\tau_\gamma \sim 4d/\eta V_s$, where η is the probability of phonon transmission at the interface and V_s is the phonon velocity.[12]

In the opposite limit, i.e., $\tau_\gamma \ll \tau_B$, $\Lambda \sim (D\tau_R)^{1/2}$ is determined by the quasiparticle recombination time

$\tau_R \equiv 1/2n_{qT}R$. It is easy to see that l_T is actually shorter than Λ in this limit. Since a local thermal equilibrium between the quasiparticle subsystem and the phonon subsystem clearly cannot be established when $\tau_\gamma \ll \tau_B$, it is a clear indication of the invalidity of the classical heat-diffusion equation in this situation.

In real experimental situations, the illumination boundary is not absolutely sharp. It is usually limited by the spherical aberration and/or the diffraction limit of the lens used. It is intuitively clear that the transition width must be larger than both 2Λ and the width of the blurred illumination boundary. There is no universal formula to determine the transition width in the general case. However, numerical calculation of some simple situations indicates that the transition width, for example, 10—90% of the full illumination level, can be roughly given by $(4\Lambda^2+W^2)^{1/2}$, where W is the width of the blurred illumination boundary.

B. Experiment

To experimentally measure the properties of the optically created interface, a 300-Å-thick 1.5-mm-wide Al film was evaporated onto a 250-μm-thick crystalline quartz substrate (z-cut) in an O_2 partial pressure of 4×10^{-4} Torr. The surface of the Al film was then oxidized in air prior to evaporation of a relatively thick (2000 Å) and narrow (25 μm) Pb counterelectrode across the Al film to form a tunnel junction. The sample was mounted vertically in an optical immersion Dewar. A simple optical pattern projection system, shown in Fig. 1, was used to create a movable half-bright and half-dark pattern on the sample plane. By taking advantage of the fact that the Al was semitransparent, another lens was used on the other side of the film to project both the sample and the illumination pattern onto a distant wall so that the sharpness of the focus and the relative position of the illumination pattern with respect to the sample could be determined. For this particular optical setup, an estimate of 5-μm optical resolution is achievable with a field size about 3 mm in diameter. The dark-to-bright edge pattern was illuminated onto the Al film through the transparent substrate with the light boundary parallel to the narrow Pb counterelectrode. Figure 2 shows a series of dI/dV-versus-V curves of the tunnel junction as the illumination boundary moved across the Pb probe. The light intensity was adjusted so that a small but observable Al superconducting gap remained when the tunneling area was fully illuminated. The superconducting gap of Pb was hardly affected by the illumination because its T_c was much higher, the film was much thicker, and the amount of light received through the semitransparent Al film was much less ($\lesssim$4% of the incident light intensity). One can see from Fig. 2 that the dI/dV curve changes completely from dark dI/dV to fully illuminated dI/dV within 30 μm of movement of the illumination boundary. Given the fact that the width of the Pb probe was 25 μm, this is certainly consistent with the estimated 5-μm optical resolution due to the lens. Furthermore, the dI/dV curves for the illumination boundary inside the tunnel area are quite different from either thermal equilibrium dI/dV curves at any temperature or the fully illuminated dI/dV curves

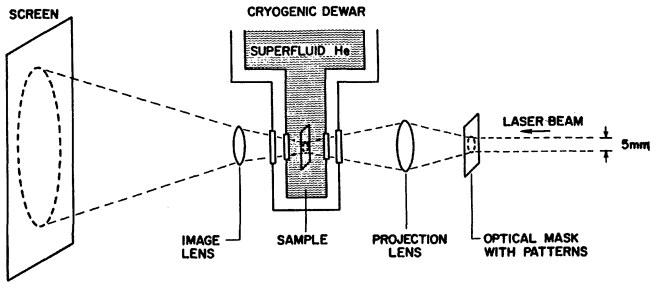

FIG. 1. A schematic representation of the experimental setup. The front projection lens (Nikkor-P, 1:4, f-105 mm) is mounted on an X-Y-Z stage (not shown) to allow precise focusing and beam positioning. The optical mask with the desired pattern is mounted on an X-Y stage (not shown) perpendicular to the direction of the laser beam so that the projection pattern can be shifted arbitrarily with respect to the sample.

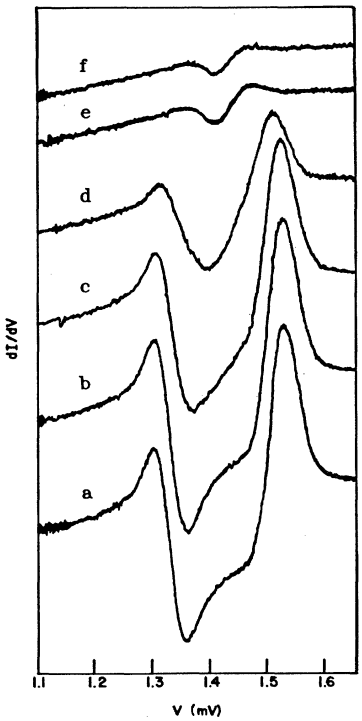

FIG. 2. dI/dV-vs-V curves as a sharp dark-to-bright edge moves across the Al film. The illumination edge is parallel to the narrow (25-μm) Pb counterelectrode. For curves a—f, the illumination edge is shifted by 10-μm steps. Curve a represents the thermal equilibrium case when the tunneling region is completely in the dark side. The peak at the higher voltage corresponds to the sum of the Al and Pb superconducting gaps. Curve b represents the case when the illumination edge almost touches the junction edge. The fact that curve b is nearly identical to curve a is indicative of a sharply focused illumination edge. Curves c and d represent the cases when 8 and 18 μm of the total 25-μm-wide tunneling region were illuminated respectively. Roughly speaking, curves c and d correspond to the dI/dV curves for an inhomogeneous junction with a larger gap, as shown in curves a and b, and a smaller gap, as shown in curves e and f which represent the case when the tunneling region is completely in the illuminated side.

for any light intensity. It is indicative of an inhomogeneous gap induced by the illumination boundary. The fact that we still could observe the dark gap when only 7 μm of the total 25-μm-wide tunneling region was on the dark side (see trace *d* of Fig. 2) strongly suggests that the total gap smearing was less than 7 μm.

To estimate the width of the dynamic interface for an absolutely sharp illumination, the mean free path l of electrons in the Al film was obtained from the resistivity measurement at 4.2 K. With $\rho l = 9\times10^{-16}$ $\Omega\,m^2$ and $\rho = 4\times10^{-7}$ Ω m, l is estimated to be 2.3 nm.[13] Using Eq. (10) with $D = V_F l/3$, $V_F = 2.0\times10^6$ m/s,[14] and $\tau_R^{\rm eff} \equiv (2n_{qT}R^{\rm eff})^{-1} \approx 1$ ns at $T \approx T_c$, we obtained $2\Lambda \approx 2.6$ μm, which is considerably smaller than our optical resolution. It was unfortunate that we could not measure 2Λ directly with the present optical setup. But this calculation indicates that at most, we can make only a factor of 2 improvement with better lenses.

Note that the thermal heating length for our Al film, estimated from Eq. (12), gives $l_T \approx 0.3$ μm $\ll \Lambda$. Therefore we conclude that the classical heat-diffusion model is not appropriate for thin Al films immersed in liquid He.

III. PROBING INHOMOGENEITY OF TUNNEL JUNCTIONS

The same sample described in Sec. II was also used to demonstrate that the optical probing technique can be a very useful tool to obtain information about the inhomogeneity of tunnel junctions.

A. Inhomogeneity of the Al film and the tunnel barrier

A short dark-bridge pattern, shown in Fig. 3, was used to probe both the Al film and the tunnel junction. The shaded area represents the dark region. The light intensity was adjusted so that the illuminated part was completely driven into the normal state at the ambient temperature. It is clear that with current and voltage leads attached to the Al film, one can measure the superconducting transition temperature T_c and the critical current I_c of the Al film as functions of the projected bridge position. The results are shown in Figs. 4(a) and 4(b). It is interesting to note that the T_c distribution has sharp peaks at both edges of the Al film. Since the Al film was deposited onto the substrate through a metal mask, it is quite conceivable that the edges were tapered due to partial shadowing. For Al films, thinner or dirtier regions usually give higher T_c's. The critical current distribution, shown in Fig. 4(b), was measured at an ambient temperature T ($\approx 0.9T_c$) reasonably close to the T_c of the Al film, so the Ginzburg-Landau mean-field theory is valid. One can use the following expression for $I_c(x)$:

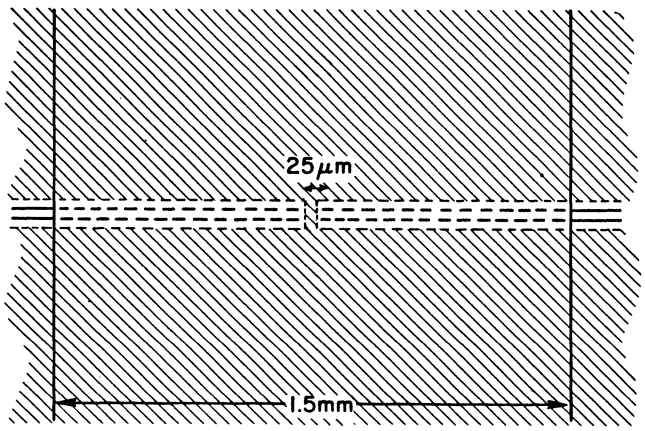

FIG. 3. A dark-bridge pattern used to probe the spatial distribution of the superconducting parameters of the Al film as well as the Josephson critical current. The dark bridge scans from one edge of the Al to the other across the tunneling region between the heavy dotted lines shown.

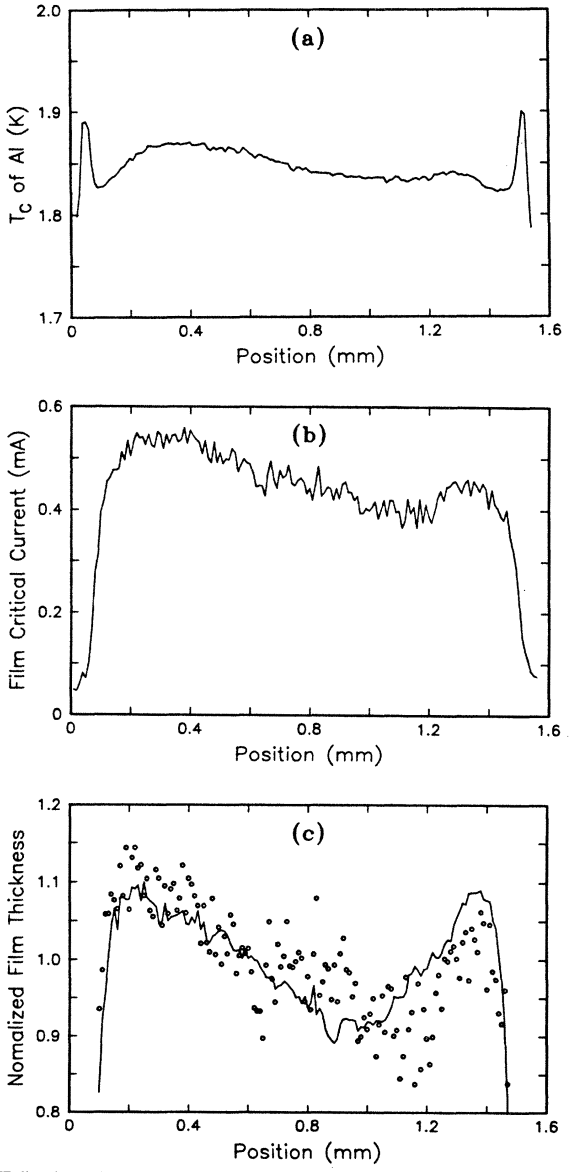

FIG. 4. Moving the projected pattern of Fig. 3 on the Al film, we obtained the following: (a) superconducting transition temperature T_c of the Al film as a function of position. (b) Critical current I_c of the Al film as a function of position. (c) Film thickness as deduced from (a) and (b) and Eq. (13) (circles), together with film thickness by optical transmissivity measurement.

$$I_c(x) \propto [1-T/T_c(x)]^{3/2} d(x) , \quad (13)$$

where $d(x)$ is the film thickness at position x along the tunneling area.

The absence of sharp peaks at both edges for the critical current distribution indicates that the film is indeed much thinner at the edges where the T_c is higher. The film thickness profile can be deduced from Eq. (13) with the measured $I_c(x)$ and $T_c(x)$. The thickness calculated is shown as circles in Fig. 4(c). To check the validity of the probing technique, the relative film thickness was independently obtained from the optical transmissivity measurement near the tunneling area. The result is shown as a solid line in Fig. 4(c). The good agreement between the two independent measurements strongly supports the probing technique and the validity of Eq. (13).

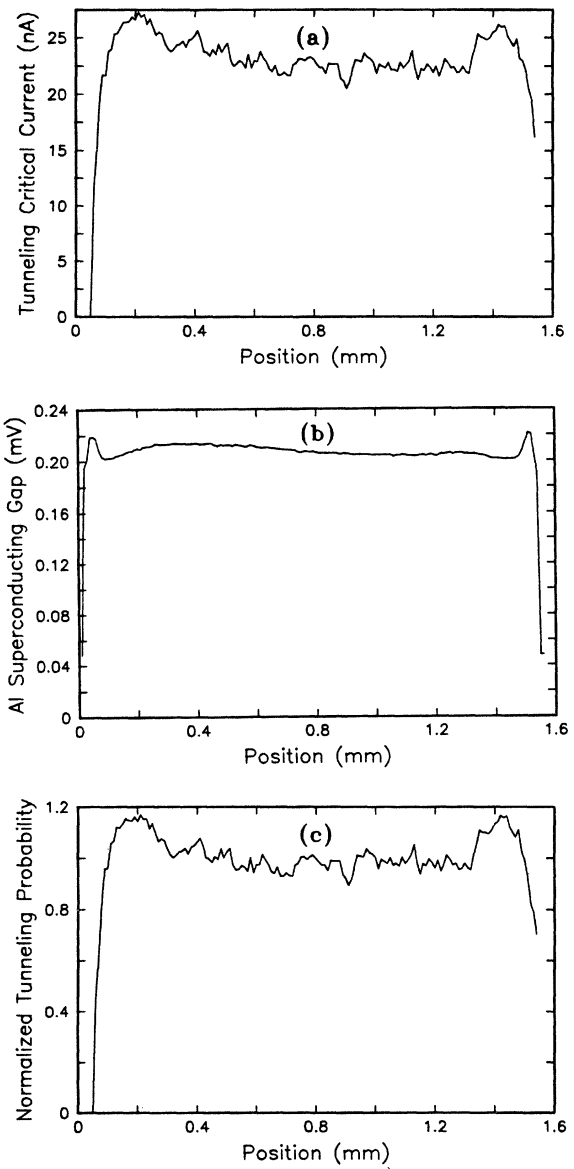

FIG. 5. (a) Local critical Josephson current $I_{JC}(x)$ as a function of position by moving the projected pattern of Fig. 3 on the tunnel junction. (b) Superconducting gap of Al as calculated from $T_c(x)$ and BCS relationship. (c) Tunneling probability as a function of position as calculated from Eq. (14) by using (a) and (b).

With the same bridge pattern, but with the current and voltage leads connected across the tunnel junction, we also measured the distribution of the critical Josephson currents $I_{JC}(x)$ shown in Fig. 5(a). Since only the dark part of the Al film can support a Josephson current, the measured $I_{JC}(x)$ is the equilibrium value of the local Josephson current without any complication due to nonequilibrium phenomena. With the dark-bridge pattern, the effective Josephson tunneling area is 25×25 μm, far less than the Josephson penetration length estimated for this junction (≈1 mm) so that a uniform supercurrent tunneling is guaranteed.

It is well known that the Josephson critical current for a small tunnel junction with extremely asymmetric gaps is given by[15]

$$I_{JC} \cong \pi\Delta/2eR_{NN} , \quad (14)$$

where Δ is the smaller gap and R_{NN} is the tunneling resistance when both electrodes are in the normal state. This is certainly a good approximation for our present case where the superconducting Pb gap is at least 5 times larger than the Al gap in our experimental temperature range (1.4–2 K).

The Al fim is known to be a very good BCS superconductor. With the measured T_c distribution and the assumed BCS relationship between the superconducting gap and T_c, a distribution of Al gaps, $\Delta(x)$, at $T=1.45$ K was obtained and is shown in Fig. 5(b). By using Eq. (14) and $I_{JC}(x)$ and $\Delta(x)$, the relative tunneling probability, which is proportional to R_{NN}^{-1}, was obtained. The result is shown in Fig. 5(c). We note that the tunneling probability is quite uniform throughout the whole length of the tunnel junction. This implies that the thickness of the tunnel barrier is extremely uniform on the scale of our probe dimension. The uniformity of the barrier thickness deduced from the relative tunneling probability is actually much better than the uniformity of the Al film itself. This is an interesting but probably not surprising conclusion for Al tunnel junctions.[16]

B. Spatial distribution of excess quasiparticle tunneling currents

A bright rectangular spot shown in Fig. 6(a), which is complementary to the dark bridge in the tunneling area, was used to probe the excess quasiparticle tunneling currents due to laser illumination. With this pattern and the tunnel junction biased at a finite voltage less than $(\Delta_{Pb}-\Delta_{Al})/e$, the distributions of the excess quasiparticle current were measured for several incident laser powers, as shown in Fig. 6(b). It is evident from this figure that the distributions of the excess quasiparticle current have much larger spatial variations than the Josephson critical current distribution obtained with a dark-bridge pattern. The lack of similarity between the two seems to be contradictory at first sight, because both the Josephson and quasiparticle tunneling current were expected to be proportional to the single-electron tunneling probability. Actually there is no serious discrepancy between them as one

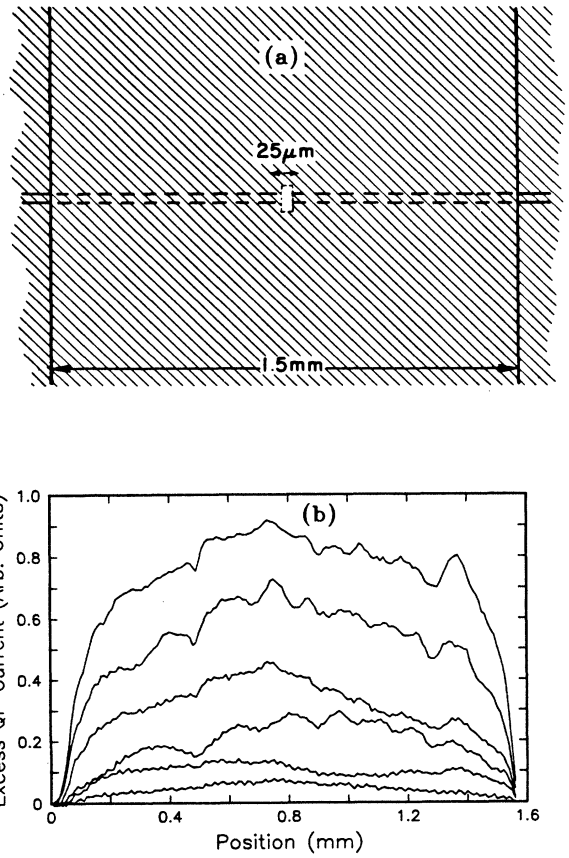

FIG. 6. (a) Bright rectangular spot mask pattern, complimentary to that shown in Fig. 3. (b) Spatial distribution of excess quasiparticle current for several incident powers as measured by projecting the pattern of (a) on the tunneling area. The incident laser intensities were measured to be 230, 160, 80, 40, 20, and 10 mW/cm^2 for the curves from the top to the bottom, respectively.

examines the detailed dependence of excess quasiparticle currents as discussed in the following paragraph.

In order to understand the excess quasiparticle current due to the laser illumination in more detail, the quasiparticle tunneling current can be written as

$$I_{\rm qp}=\frac{1}{eR_{\rm NN}}\int_{-\infty}^{\infty} dE\,\rho_{\Delta_1}(E)\rho_{\Delta_2}(E+eV) \times[f_1(E)-f_2(E+eV)]\,, \tag{15}$$

where $\rho_\Delta(E)=|E|/(E^2-\Delta^2)^{1/2}$ for $|E|>\Delta$ and 0 otherwise. For the present experiment, we have $\Delta_2\gg\Delta_1$, and $f_2(E)\approx 0$ because $\Delta_2\gg k_BT$ and the second film (Pb) is not directly illuminated. Then the excess current due to illumination on the Al film can be written as

$$\delta I_{\rm qp}=\frac{1}{eR_{\rm NN}}\int_{-\infty}^{\infty} dE\,\rho_{\Delta_1}(E)\rho_{\Delta_2}(E+eV) \times\left[\delta f_1(E)+f_1(E)\frac{\Delta_1^2}{E^2-\Delta_1^2}\frac{\delta\Delta_1}{\Delta_1}\right]. \tag{16}$$

Using the BCS gap equation, one can relate $\delta\Delta_1/\Delta_1$ to $\delta f_1(E)$ as follows:

$$\delta\Delta_1/\Delta_1=[\delta n_q/2N(0)\Delta_1]\langle\Delta_1/E\rangle_{\delta f_1}\,, \tag{17}$$

where δn_q is the excess quasiparticle density and

$$\langle\Delta_1/E\rangle_{\delta f_1}\equiv\left[\int_{-\infty}^{\infty}\rho_\Delta(E)dE\,\delta f_1(E)(\Delta_1/E)\right]\Big/\delta n_q\,.$$

One can see, from Eqs. (16) and (17), that the excess quasiparticle current depends not only on the total excess quasiparticle density but also the excess quasiparticle energy distribution.

Furthermore, the steady-state value of the excess quasiparticle density depends sensitively on the local light intensity and energy relaxation rates, i.e., electron-phonon inelastic scattering rate, phonon-thermal bath thermalization rate etc. There are clear maxima and minima in Fig. 6(b), which are not related to noise in the measurements; the critical Josephson currents measured with the dark-bridge pattern do not show the corresponding variations. Thus we believe that the variation in the excess quasiparticle currents is not due to the inhomogeneity in the tunnel barrier, it is most likely due to the spatial variation in τ_γ. For example, an ice particle on the surface could decrease the phonon-escape rate from the film with a corresponding increase in the excess quasiparticle current due to the light illumination. Therefore, we conclude that one cannot extract the information about the tunneling probability from the excess quasiparticle current distribution unless one can assume the uniformity of various relaxation processes. The present experiment clearly demonstrates that it is a poor assumption, at least for this particular sample.

IV. CONCLUSION

We have demonstrated that dynamic S-N or S-S' interfaces can be generated by patterned laser illumination of superconducting films. The dynamic interface has a maximum width due to quasiparticle diffusion. The length scale of the width is approximately 2Λ [Eq. (10)]. Depending upon the light intensity and ambient temperature, the excess quasiparticle density changes from the illuminated side to the dark side with either an exponential or a power-law relationship. The classical thermal healing length l_T [Eq. (12)], is the limiting value of Λ when the phonon-escape time τ_γ is much longer than the phonon pair-breaking time τ_B. In practice, for a typical optical projection system such as the one used in this experiment, the optical resolution is of the order of a few microns. For a thin Al film (300 Å), the calculated value for Λ is of the same order of magnitude but slightly smaller. Therefore for the present experiment, the interface width is largely limited by the optical resolution rather than quasiparticle diffusion length. The experimental result of the dI/dV curves of a Al-Al_2O_3-Pb junction as a sharp illumination edge is passed through the junction region clearly demonstrates that the total spatial resolution of our system is about 5 μm.

Using this versatile projection technique, we have used a simple dark-bridge pattern to measure the T_c and I_c

distributions of the Al film, and the critical Josephson current I_{JC} of the Al-Al_2O_3-Pb junction. From these measurements, we are able to obtain the thickness distribution of the Al film, which is in very good agreement with the result obtained from optical transmissivity measurements. For the first time, we are also able to obtain the distribution of the tunneling probability, which is reasonably flat as expected for a good-quality Al junction.

With a bright rectangular spot pattern, which is complimentary to the dark-bridge pattern used, we also measured the distributions of the excess quasiparticle current for several light intensities. The excess quasiparticle current shows much more spatial variation than either the critical Josephson current distribution or the tunneling probability distribution. We have shown that the excess quasiparticle current is inherently a nonequilibrium process. Its steady-state value would sensitively depend on the phonon thermalization process, quasiparticle-phonon inelastic scattering, as well as the tunneling probability of the tunnel barrier. Therefore, the tunneling probability extracted from the critical Josephson current distribution should be much more reliable.

Finally, it is worthwhile to point out that one would have a much wider experimental temperature range if the sample were cooled by He vapor or by a cold contact finger instead of being immersed in superfluid helium. However, the penalty one is likely to incur is the increase in the quasiparticle diffusion length, which makes the drive for higher optical resolution unwarranted.

Note added in proof. An analytic solution of the nonlinear diffusion equation [Eq. (7)] has been found as follows:

$$n_q(x)=n_{q-}+3n_{q-}/\sinh^2[(n_{q-}R^{\text{eff}}/2D)^{1/2}\,|x|+C_-] \quad \text{for } x<0\,,$$

$$n_q(x)=n_{q+}-3n_{q+}/\cosh^2[(n_{q+}R^{\text{eff}}/2D)^{1/2}\,|x|+C_+] \quad \text{for } x>0\,,$$

where

$$C_-=\tfrac{1}{2}\ln\left[\frac{[n_q(0)+2n_{q-}]^{1/2}+(3n_{q-})^{1/2}}{[n_q(0)+2n_{q-}]^{1/2}-(3n_{q-})^{1/2}}\right],$$

$$C_+\equiv\tfrac{1}{2}\ln\left[\frac{(3n_{q+})^{1/2}+[n_q(0)+2n_{q+}]^{1/2}}{(3n_{q+})^{1/2}-[n_q(0)+2n_{q+}]^{1/2}}\right],$$

$$n_q(0)=2(n_{q-}^2+n_{q-}n_{q+}+n_{q+}^2)/3(n_{q-}+n_{q+})\,.$$

It is interesting to note that the quasiparticle density at the illumination boundary, $n_q(0)$, varies from $(n_{q-}+n_{q+})/2$ to $2n_{q+}/3$ for the weak- to the strong-illumination limit. The approximate solutions for the weak- and strong-illumination limits, Eqs. (9) and (11), are the natural consequences of the general solution given as above.

ACKNOWLEDGMENTS

We thank J. C. Dohm for making projection masks for this experiment, and Dr. R. B. Laibowitz for critically reading the manuscript. The work of one of us (M.M.T.L.) was partially supported by the U.S. Office of Naval Research.

[1]For an example, *Nonequilibrium Superconductivity, Phonons, and Kapitza Boundaries,* edited by K. E. Gray (Plenum, New York, 1981).

[2]C. C. Chi, M. M. T. Loy, and D. C. Cronemeyer, Appl. Phys. Lett. 40, 437 (1982).

[3]M. Scheuermann, J. R. Lhota, P. K. Kuo, and J. T. Chen, Phys. Rev. Lett. 50, 74 (1983).

[4]P. L. Stöhr and R. P. Huebener, J. Low Temp. Phys. 37, 277 (1979).

[5]R. Eichele, H. Seifert, and R. P. Huebener, Appl. Phys. Lett. 38, 383 (1981).

[6]P. L. Stöhr, Appl. Phys. Lett. 39, 828 (1982).

[7]P. W. Epperlein, H. Seifer, and R. P. Huebener, Phys. Lett. 92A, 146 (1982).

[8]W. J. Skocpol, M. R. Beasley, and M. Tinkham, J. Appl. Phys. 45, 4054 (1974).

[9]A. Rothwarf and B. N. Taylor, Phys. Rev. Lett. 19, 27 (1967).

[10]C. C. Chi, Ph.D. thesis, University of Pennsylvania, Philadelphia, 1976 (unpublished).

[11]C. C. Chi, M. M. T. Loy, and D. C. Cronemeyer, Phys. Rev. B 23, 124 (1981).

[12]G. A. Sai-Halasz, C. C. Chi, A. Denenstein, and D. N. Langenberg, Phys. Rev. Lett. 33, 215 (1974).

[13]F. R. Fickett, Cryogenics 11, 349 (1971).

[14]C. Kittel, *Introduction to Solid State Physics,* 5th ed. (Wiley, New York, 1976), p. 154.

[15]V. Ambegaokar and A. Baratoff, Phys. Rev. Lett. 10, 486 (1963); 11, (E)104 (1963).

[16]Al film is well known for its capability of growing thermal oxide. Recently, there was a report of successfully fabricating all Nb junctions using Al oxide as the tunnel barrier [M. Gurvitch, M. A. Washington, H. A. Higgins, and J. M. Rowell, IEEE Trans. Mag. MAG-19, 791 (1983)].